

Long-wave Infrared Computational Multispectral Metasurface and Spectral Reconstruction Method: supplemental document

1. STRUCTURE AND PRINCIPLE

By adjusting the lattice constant and pore size of photonic crystals, bandgaps may be produced within a specific wavelength range. Some studies have shown that within the bandgap range, adjusting the structural dimensions can filter out light of specific wavelengths [?]. In order to achieve wideband transmission, this research aims to circumvent these bandgap regions within a specific wavelength range by mapping the position and size of photonic bandgaps in various two-dimensional photonic crystals. The photonic bandgap position map of the crystal is obtained by scanning either the ratio of pore radius (r) to lattice constant (a) or the ratio of thickness (h) to lattice constant (a). This mapping illustrates the bandgap of square and triangular lattice photonic crystals. We will simulate the band structure of air columns in a dielectric substrate, where the dielectric constant ratio is 13.7:1. In Fig. 1 (a), the vertical axis represents the normalized angular frequency, and the horizontal axis represents $R = r/a$. The TE and TM polarizations are plotted together in Fig. 1 (b), with the bandgap diagram of the two-dimensional photonic crystal shown below. In the band diagram, the green region represents the selected position of the normalized frequency (a/λ). Additionally, for triangular lattices at angles of 0 degrees, 45 degrees, and 60 degrees (or 30 degrees), the TE/TM band gaps were obtained.

After obtaining the bandgap diagrams, we identified regions without TE and TM bandgaps within the two-dimensional photonic crystal slab. The bandgap diagram is shown in Fig. 1, indicating a significant bandgap in the normalized frequency range of 0.2-0.55, from $\omega a/2\pi c = 0.207$ to $\omega a/2\pi c = 0.554$. To convert these dimensionless numbers into physical units, we want the working wavelength $\lambda = 2\pi c/\omega$ in the range of 8-11.5 μm to be located in the gapless region. When $R = 0.326$ -0.654, the gapless region must satisfy:

$$\omega a/2\pi c = a/\lambda = a/8\mu m - a/11.5\mu m = 0.207 - 0.551. \quad (S1)$$

The normalized frequency ($\omega a/2\pi c = a/\lambda$) is typically in the range of 0.2-1.2, which is more suitable for modulating the optical field. In photonic crystals, the long-wave infrared range of 8-11.5 μm is modulated by periodic structures to control photon transitions. By adjusting the duty cycle $R = r/a$ or the lattice constant, regions without band gaps within the 8-11.5 μm range can be selected.

The photonic crystal slab made up of a 3×3 array of photonic crystals of varying sizes. As shown in Table 1, the area enclosed by the transmission spectra and the wavelength axis, representing the energy utilization rate, ranges from 21.4% to 47.2%, with an average of 32.7% and 49.37%. The peak transmittance can reach up to 90%, with an average peak value of 70%. The bandwidth of the narrowband filter is less than 5% of the central wavelength, and the energy utilization rate of a single filter is approximately in the range of 5% to 15% [1], [2]. Compared to typical narrowband filters, the energy utilization rate per unit area is more than double that of standard narrowband filters.

2. SPECTRUM RECONSTRUCTION

During the training of the network, a predetermined transmission matrix with fixed parameters is used to predict the reconstructed spectral response of the structure. It is noteworthy that the loss function is derived from the least squares between the input and the reconstructed spectrum. Thus, different transmission matrix parameters yielding similar spectral responses will no longer cause confusion, significantly enhancing the prediction accuracy of the neural network. At the same time, the statistical distribution of mean absolute error (MAE) and loss function value of the

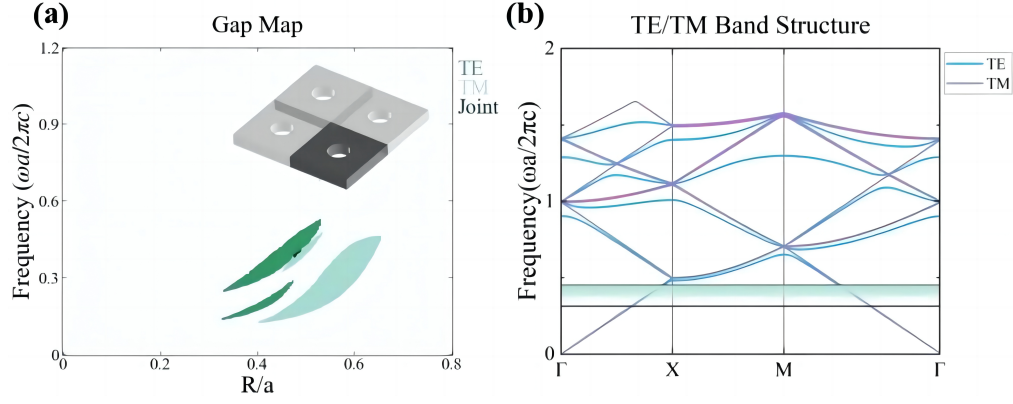


Fig. S1. The gap maps and band maps of photonic crystal slab. (a) The bandgap maps of photonic crystals. (b) Energy band diagram.

Table S1. Parameters and Energy Utilization Rates of The First Group of Photonic Crystal Slab

Photonic Crystal Sequence	Lattice Constant a (μm)	Hole Radius r (μm)	Slab Thickness h (μm)	Lattice Arrangement Angle ($^\circ$)	Energy Utilization Rate (%)
a	5.75	1.9	1.89	0	47.22
b	5.75	2.09	1.89	0	45.60
c	4.4	0.89	1.89	0	30.30
d	3.6	0.7	1.89	0	32.57
e	4.4	1.2	1.89	0	33.04
f	4.4	0.98	1.89	0	32.06
g	10	0.99	1.89	30	28.16
h	12	1.53	1.89	45	23.59
i	5.806	1.307	1.89	60	21.35

reconstructed spectra and actual spectra of two groups of different photonic crystal arrays were calculated. The mean square error (MSE) between the reconstructed spectrum and the actual spectrum is defined as follows:

$$MSE = \frac{1}{k} \sum_{i=1}^k (I_i - \tilde{I}_i)^2. \quad (\text{S2})$$

Where k represents the number of discrete data points in the transmission spectrum, which is 201. I_i denotes the true values of the incident spectrum, and \tilde{I}_i represents the spectrum values reconstructed by the network model.

The low loss values indicate that the training process of Bp performed well in Fig. 8(a). After training, the specific error distribution of the test dataset was analyzed. Fig. 8(b) and Fig. 8(c) compare the results, showing the relationship distribution between the predicted reconstructed spectrum and the true values at wavelengths of 8.175 μm and gamut. Here, MAE is used as the metric to plot the error statistical distribution curve and histogram. As shown in Fig. 8(d), it can be seen that most sample data have an MAE error below 0.08, with only 1.4% of the dataset samples having an MAE exceeding 0.05. The simulated noise is shown in Fig. 8(e). The mean squared error (MSE) of the test dataset is 1.292×10^{-3} , corresponding to a mean absolute error ($MAE = \frac{1}{k} \sum_{i=1}^k (I_i - \tilde{I}_i)^2$) of 0.0134 in Fig. 8(f).

To further illustrate the predictive performance of Bp more intuitively, we randomly selected three samples from the test set for comparison, as shown in Fig. 9. It can be seen that these

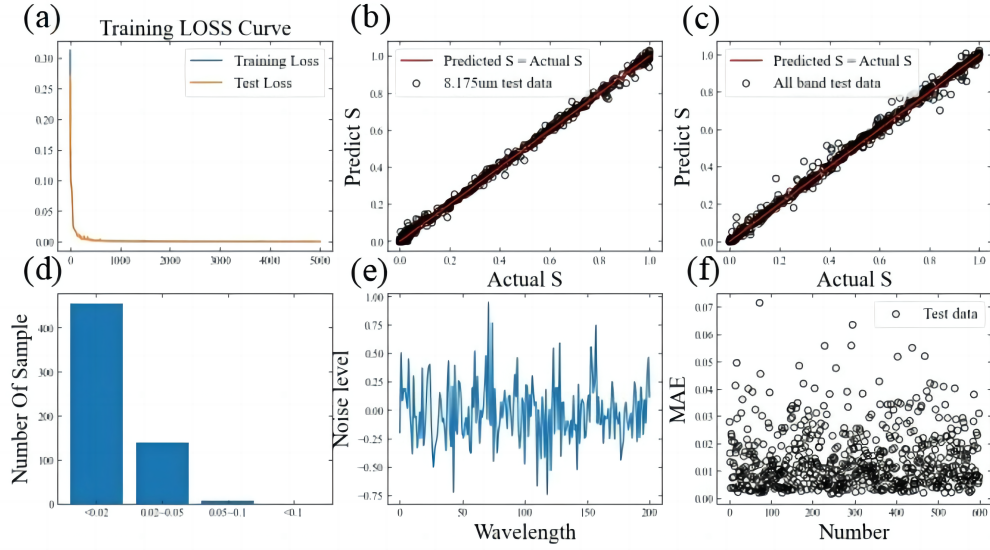


Fig. S2. The First Set of Deep Learning Results for Photonic Crystal Arrays: The top row, from left to right, corresponds to figures a to c, representing the loss function curve, the scatter plot of the reconstructed spectrum and the true spectrum at a wavelength of 8.175 μm , and the scatter plot over the entire wavelength range, respectively. The bottom row, from left to right, corresponds to figures d to f, showing the statistical distribution of test set samples within different MAE ranges, the experimental noise simulated by Gaussian white noise in the middle, and the MAE between the true spectrum and the metasurface reconstructed spectrum.

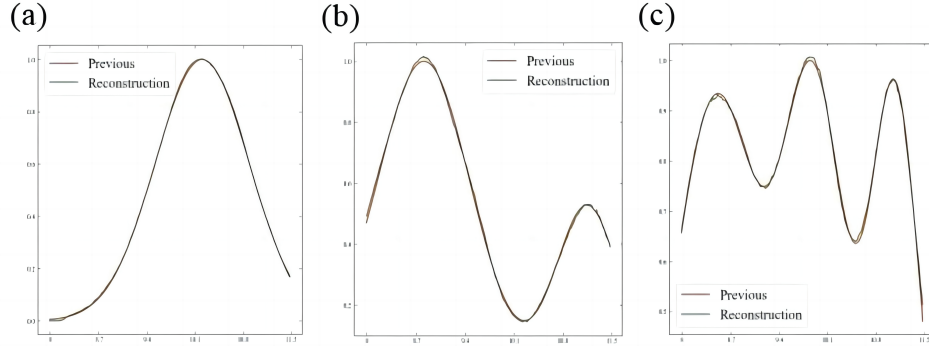


Fig. S3. Comparison of Reconstructed Spectrum and Original Spectrum.

two sets of data fit very well, which also demonstrates the superior performance of the neural network.

REFERENCES

1. M. Dong, T. Chen, Y. Xiong, *et al.*, "Design and preparation of lwir narrow-band filter with wide rejection band," *Chin. Opt. Lett.* **11**, S104011–S104013 (2013).
2. Y. Zhang, Z. Liang, D. Meng, *et al.*, "A long wavelength infrared narrow-band reflection filter based on an asymmetric hexagonal structure," *Opt. Commun.* **475**, 126264 (2020).